HHS Public Access

Author manuscript

Nature. Author manuscript; available in PMC 2009 September 26.

Published in final edited form as:

Nature. 2009 March 26; 458(7237): 501–504. doi:10.1038/nature07722.

Specific synapses develop preferentially among sister excitatory neurons in the neocortex

Yong-Chun Yu[1], **Ronald S. Bultje**[1,2], **Xiaoqun Wang**[1], and **Song-Hai Shi**[1]

[1]Developmental Biology Program, Memorial Sloan Kettering Cancer Centre, 1275 York Avenue, New York, NY 10021

[2]Department of Pharmacology, Weill Medical College of Cornell University, 445 East 69th Street, New York, NY 10065

Abstract

Neurons in the mammalian neocortex are organized into functional columns 1, 2. Within a column, highly specific synaptic connections are formed to ensure that similar physiological properties are shared by neuron ensembles spanning from the pia to the white matter. Recent studies suggest that synaptic connectivity in the neocortex is sparse and highly specific 3–8 to allow even adjacent neurons to convey information independently 9–12. How this fine-scale microcircuit is constructed to create a functional columnar architecture at the level of individual neurons largely remains a mystery. Here we investigate whether radial clones of excitatory neurons arising from the same mother cell in the developing neocortex serve as a substrate for the formation of this highly specific microcircuit. We labelled ontogenetic radial clones of excitatory neurons in the mouse neocortex by *in utero* intraventricular injection of EGFP-expressing retroviruses around the onset of the peak phase of neocortical neurogenesis. Multiple-electrode whole-cell recordings were performed to probe synapse formation among these EGFP-labelled sister excitatory neurons in radial clones and the adjacent non-siblings during postnatal stages. We found that radially aligned sister excitatory neurons have a propensity for developing unidirectional chemical synapses with each other rather than with neighbouring non-siblings. Moreover, these synaptic connections display the same interlaminar directional preference as those observed in the mature neocortex. These results suggest that specific microcircuits develop preferentially within ontogenetic radial clones of excitatory neurons in the developing neocortex and contribute to the emergence of functional columnar microarchitectures in the mature neocortex.

Recent studies have demonstrated that radial glial cells are the major neuronal progenitors in the developing neocortex 13–17. In addition to their well-characterized role in guiding the radial migration of postmitotic neurons 18, radial glial cells divide asymmetrically to self-

Correspondence and requests should be addressed to S.-H.S., Song-Hai Shi, Email: shis@mskcc.org, Tel: 212-639-5009, Fax: 212-717-3738.

Author Contributions

Y.-C. Y. and S.-H. S. conceived the experiments. Y.-C. Y. conducted the electrophysiology and imaging experiments. R. S. B and X. W. helped with *in utero* virus injection. Y.-C. Y. and S.-H. S. analysed data and wrote the manuscript.

renew and to give rise to neurons. Consecutive asymmetric cell divisions of individual radial glial cells produce a number of clonally related neurons that migrate radially into the cortical plate. This results in a columnar arrangement of neocortical neurons – the ontogenetic radial clone 13, 14, 19, 20. It has previously been suggested that "ontogenetic columns become the basic processing unit in the adult cortex" 19; however, this assertion is based largely on their anatomical similarity, i.e. the vertical arrangement of neurons. In fact, virtually nothing is known about the functional development of ontogenetic radial clones in the neocortex.

To study the functional development of ontogenetic radial clones in the developing neocortex, we injected retroviruses expressing enhanced green fluorescence protein (EGFP) through the uterus into the ventricle of mouse embryos around 12 to13 days after conception (embryonic day 12 to 13, E12–E13) (Fig. 1a) – the period during which the peak phase of neocortical neurogenesis begins. After injection, the uterus was placed back to allow the embryos to come to term. Previous studies have shown that about half of the retroviral integration events occur in the self-renewing daughter cells 21, resulting in the labelling of neocortical progenitor cells and their radially aligned clonal progeny 13, 20. Similarly, we found that intraventricular injection of a low titre EGFP-expressing retrovirus at E12–E13 reliably labelled the radial clones of cells (Fig. 1 b and c), while additionally labelling some scattered cells (data not shown) 22, 23, throughout the developing neocortex. In this study we focused our analysis on the isolated radial clones that consisted of sister cells (Fig. 1 and Supplementary Fig. S1).

In brain sections at various embryonic stages we frequently observed individual radial clones that comprised a radial glial mother cell (Fig. 1b, red arrowhead) and a cluster of additional cells (~4–6 cells per clone at E18, Fig. 1b, white arrowheads), all of which were in contact with the radial glial fibre of the mother radial glial cell. As development progressed into postnatal stages, the frequency of radial clones observed in individual brain sections decreased. Nonetheless, we often found isolated radial clones with two or more cells in individual sections that did not have any scattered cells in close proximity (Fig. 1c and Supplementary Fig. S1), suggesting that the cells in these radial clones are lineage-related sisters. Nearly all of the cells in the labelled radial clones exhibited the morphological features of an excitatory neuron – a radially oriented pyramid-shaped cell body and a major apical process that progressively branched (Fig. 1c) and harboured dendritic spines (data not shown) as they developed.

We proceeded to perform whole-cell patch clamp recordings to assess the physiological development of these ontogenetic radial clones in the developing neocortex during postnatal stages (Supplementary Fig. S2). As time progressed, the input resistance of neurons in the radial clone decreased (data not shown) and their resting membrane potential (RMP) became progressively more hyperpolarized (Supplementary Fig. S2 a and b), indicating a maturation of membrane conductance. Furthermore, as development progressed, the threshold for firing action potential decreased drastically, whereas the maximum firing rate increased significantly (Supplementary Fig. S2 c and d).

Synapse formation is a key step in the functional development of neurons in the brain. To assess synapses formed onto the excitatory neurons in ontogenetic radial clones, we

examined the spontaneous miniature excitatory postsynaptic currents (mini-EPSCs) (Supplementary Fig. S2 e–k). While the mean amplitude of mini-EPSCs detected at different developmental stages remained similar (Supplementary Fig. S2 e and f), the frequency increased drastically as development progressed (Supplementary Fig. S2 e and g). Moreover, the rise and decay of mini-EPSCs speeded up significantly with development (Fig. 2 h–k). These results suggest progressive formation and maturation of synapses onto the excitatory neurons in ontogenetic radial clones during postnatal development.

Having found that the neurons in ontogenetic radial clones actively form synapses, we set out to determine whether sister neurons in individual radial clones form synapses with each other. Simultaneous whole-cell recordings were performed on two EGFP-expressing sister neurons in individual radial clones, whose cell bodies were often more than 100 μm apart (Fig. 2a). After the recordings were established, single as well as a train of action potentials were triggered in one of the neurons by current injection, while the other neuron was kept in voltage-clamp mode around −70 mV to record postsynaptic responses (Fig. 2b). If the sister neurons are synaptically connected, action potentials triggered in the presynaptic neuron should evoke synaptic currents in the postsynaptic neuron. Indeed, we found that action potentials triggered in one neuron (neuron 1) reliably evoked postsynaptic currents in the other neuron (neuron 2, Fig. 2 a and b), indicating that these two sister neurons in a radial clone are indeed connected. Moreover, we found that the connection between them was unidirectional, as action potentials triggered in neuron 2 failed to evoke detectable postsynaptic currents in neuron 1 (Fig. 2 a and b). Similar results were obtained when the postsynaptic neuron was kept in current-clamp mode (Fig. 2c). The biophysical properties of these postsynaptic responses recorded between sister neurons in radial clones indicate that they are glutamate-receptor mediated EPSCs. This was corroborated by pharmacological experiments using picrotoxin, D-AP5, and NBQX (Fig. 2d) – the inhibitors of γ-aminobutyric acid (GABA)-A, N-methyl-D-aspartic acid (NMDA), and α-amino-3-hydroxy-5-methyl-4-isoxazolepropionic acid (AMPA) receptors, respectively, as well as carbenoxolone and 18α-glycyrrhetinic acid – two commonly used blockers of gap junctions (Supplementary Fig. S3).

Our results thus far suggest that sister excitatory neurons in individual radial clones in the developing neocortex develop unidirectional chemical synapses. We examined 101 pairs of sister neurons in individual radial clones at different developmental stages (Fig. 3e). Whereas the rate of finding a connected pair of sister neurons in a radial clone was rather low around the first postnatal week (0 out of 34 at P1–5, and 2 out of 21 at P6–9), it increased dramatically around the second postnatal week (7 out of 20 at P10–13, and 9 out of 26 at P14–17), suggesting that the second postnatal week is a critical period for the development of synaptic connections between sister neurons in a radial clone. This time window coincides with the critical period of functional circuit development in the neocortex 24–26.

Previous studies suggested that the probability of detecting a synaptic connection between adjacent excitatory neurons in the mature neocortex is between 5% to 20% depending on the neocortical layer that they are located in and the neuronal subtype 4–7, 27. Sister excitatory neurons in a radial clone in the developing neocortex are located quite far away from each

other (a hundred to few hundred μm). Therefore, the likelihood of finding a synaptic connection between them would be far lower 5. Nonetheless, we found that ~35% (16 out of 46) of sister excitatory neurons in a radial clone around P10 to P17 were connected, suggesting a propensity for radially aligned sister excitatory neurons to form synapses with each other.

To directly test this, we performed quadruple whole-cell recordings on two EGFP-expressing sister neurons in individual radial clones and two non-EGFP-expressing neurons adjacent to the EGFP-expressing sister neurons on the same side in the developing neocortex at P10–P17 (Fig. 3 a–c and Supplementary Fig. S4). We targeted non-EGFP-expressing neighbouring neurons with radially aligned pyramid-shaped cell bodies because they were most likely to be excitatory neurons and the progeny of different progenitor cells. Furthermore, the morphology and biophysical properties of these control neurons confirmed that they were excitatory neurons (Fig. 3 d–g). Hence, they served as adjacent non-sibling controls. Once all four recordings were established, action potentials were sequentially triggered in one of the four neurons and the postsynaptic responses were then measured in the other three neurons to probe synapses formed among them. As shown in Fig. 3 d–e, when action potentials were triggered in EGFP-expressing neuron 1, glutamate receptor-mediated EPSCs were recorded only in its sister neuron 3 (Fig. 3 d and e). And despite the nearly complete overlap of the dendritic arbours of adjacent neurons 3 and 4 (Fig. 3g), no EPSC was detected in the non-sibling neuron 4 (Fig. 3d). Furthermore, action potentials triggered in all three remaining neurons (neuron 2, 3 and 4) failed to evoke any detectable EPSCs in the other three neurons (Fig. 3d). These results suggest that a unidirectional synaptic connection selectively develops between two sister excitatory neurons, but not between non-sisters, in the developing neocortex (Fig. 3g).

We analyzed a total of 179 pairs of radially aligned EGFP-expressing sister excitatory neurons and their neighbouring non-sibling neurons (Fig. 3h). Among them, 36.9% (65 out of 179) of sister neurons in a radial clone were connected. By contrast, only 6.3% (9 out of 143) of radially situated non-sister excitatory neurons (one EGFP-expressing and one non-EGFP-expressing) were connected (Fig. 3h). These results clearly suggest that sister excitatory neurons in a radial clone have a strong preference to form synapses with each other rather than with adjacent non-sister neurons, and the rate of connectivity between distant, radially situated non-sister excitatory neurons is rather low. Consistent with this low rate of connectivity, only 5.5% (4 out 73) of any two randomly selected radially situated non-EGFP-expressing neurons over at least 100 μm apart were connected (Fig. 3h).

Previous studies have revealed the overall organization of the excitatory neuron microcircuit in the mature neocortex 28, 29. Thalamic input enters primarily into layer 4 (the first station of sensory processing). Layer 4 excitatory neurons send ascending projections to pyramidal neurons in layer 2/3 (the second station of columnar processing), which provide a prevalent descending projection to layer 5/6 pyramidal neurons (the third station of columnar processing). Descending and ascending excitatory connections also exist between layer 4 and layer 5/6. In addition to the sister neurons radially situated in layer 2/3 and layer 5/6 (Fig. 3 a–g), our dataset of quadruple recordings contained radially aligned sister neurons located in layer 4 and layer 5/6 (Fig. 4 a and b, and Supplementary Fig. S5a) as well as in

layer 2/3 and layer 4 (Fig. 4 c and d, and Supplementary Fig. S5b). These experiments allowed us to address the interlaminar direction preference of synaptic connectivity formed within ontogenetic radial clones of excitatory neurons. We found that 15 out of 21 connected sister excitatory neuron pairs located in layer 2/3 and layer 5/6, and 10 out of 14 pairs of those located in layer 4 and layer 5/6 formed synapses in the descending direction (i.e. from layer 2/3 to layer 5/6 and from layer 4 to layer 5/6), whereas 15 out of 19 pairs of connected sister excitatory neurons located in layer 2/3 and layer 4 formed synapses in the ascending direction (i.e. from layer 4 to layer 2/3, Fig. 4 e and f). These results suggest that the synaptic connection formed among sister excitatory neurons in ontogenetic radial clones is rather specific. Moreover, these results demonstrate that the specificity of synaptic connectivity formed within ontogenetic radial clones of excitatory neurons in the developing neocortex is highly similar to that in the mature neocortex.

The concept of the column has cast a dominant influence on our understanding of the functional organization of the neocortex 1, 2. From its inception, the concept of the functional column has been considered on both a macroscopic as well as a microscopic scale. However, most of our knowledge about functional columns and neocortical maps comes from measurements with limited spatial resolution. Recent *in vivo* Ca^{2+} imaging studies elegantly demonstrated that even adjacent neurons can have distinct physiological properties 9–11, indicating that neocortical maps are built with single-neuron precision. In this study, we found that sister excitatory neurons in individual radial clones in the developing mouse neocortex preferentially develop highly specific synaptic connections with each other, creating radial columnar microarchitectures of interconnected neuron ensembles with single-neuron resolution. The high degree of similarity in the direction of interlaminar connectivity between the synapses formed within individual ontogenetic radial clones and those observed in the mature neocortex suggests that these radial clones contribute to the formation of precise functional columnar architectures in the neocortex. Along this line, variations in the neurogenesis and emergence of ontogenetic radial clones during early neocortical development 30 may underlie differences that have been observed in the functional organization of the mature neocortex across species 10.

Methods Summary

Replication-incompetent EGFP-expressing retroviruses (a kind gift from Dr. Noctor and Dr. Gage) were intraventricularly injected into E12–13 mouse embryos as previously described 13. Acute cortical slices were prepared at different postnatal stages. Multiple-electrode whole-cell recordings were performed onto EGFP-expressing neurons in individual radial clones and their near neighbours under visual guidance of epi-fluorescence and infra-red differential interference contrast (IR-DIC) illumination. Recordings were collected and analyzed using Axopatch 700B amplifier and pCLAMP10 software (Molecular Devices) and Igor 5 software (Wavemetrics Inc). The morphology of neurons was reconstructed with confocal laser scanning microscopy using FluoView (Olympus), Neurolucida (MicroBrightField Inc) and Photoshop (Adobe Systems). Data were presented as mean ± s.e.m. and statistical differences were determined using nonparametric Mann-Whitney-Wilcoxon test.

Online Methods

Retroviral infection

Replication-incompetent enhanced GFP-expressing retrovirus was produced from a stably transfected packaging cell line (293 gp NIT-GFP; a kind gift from Dr. Noctor and Dr. Gage) as previously published 15. Animals were maintained according to protocols approved by the Institutional Animal Care and Use Committee at the Memorial Sloan Kettering Cancer Centre. Uterine horns of E12–E13 gestation stage pregnant CD-1 mice (Charles River Laboratories, MA) were exposed in a clean environment. Retrovirus (~1.0 μl) with Fast green (2.5 mg/ml, Sigma) was injected into the embryonic cerebral ventricle through a bevelled, calibrated glass micropipette (Drummond Scientific, Broomall, PA). After injection, the peritoneal cavity was lavaged with ~10 ml warm phosphate buffered saline (PBS, pH 7.4) containing antibiotics, the uterine horns were re-placed, and the wound was closed.

Electrophysiology

Embryos that received retroviral injections were delivered naturally. Brains were removed at different postnatal days and acute cortical slices were prepared at ~300 μm in artificial cerebral spinal fluid (ACSF) containing (in mM) 126 NaCl, 3 KCl, 1.25 KH_2PO4; 1.3 $MgSO_4$, 3.2 $CaCl_2$, 26 $NaHCO_3$, and 10 glucose, bubbled with 95% O_2/5% CO_2) on a Vibratome at 4° C (Leica Microsystems). Slices were first recovered in an interface chamber at 35° C for at least one hour and then kept at room temperature before being transferred to a recoding chamber containing ACSF at 34° C. An infrared-differential interference contrast (DIC) microscope (Olympus) equipped with epifluorescence illumination, a CCD camera, and two water immersion lenses (10x and 60x) were used to visualize and target recording electrodes to EGFP-expressing sister cells in radial clones and their nearby control cells. Glass recording electrodes (7–9 MΩ resistance) were filled with an intracellular solution consisting of 130 mM K-gluconate, 6 mM KCl, 2 mM $MgCl_2$, 0.2 mM EGTA, 10 mM HEPES, 2.5 mM Na_2ATP, 0.5 mM Na_2GTP, 10 mM K-phosphocreatine and 0.5% Alexa 546-conjugated biocytin (Invitrogen) (pH 7.25 and 295 mOsm/kg). All recordings had access resistance less than 30MΩ. In all dual, triple, and quadruple recordings, connections between neuron pairs were assessed by injecting current to evoke action potentials in one of the cells kept in current-clamp while testing for postsynaptic responses in other cells during voltage-clamp recording at −70 mV unless specified. For every possible pair, connections were tested in both directions for at least 20 trials, with both single and trains of action potential being generated in each presynaptic neuron. In some experiments, Picrotoxin (50 μM), D-AP5 (50 μM), and NBQX (10 μM) (Tocris Biosciences, MI) were added to the bath to block GABA-A, NMDA, and AMPA receptors, respectively. Carbenoxolone (100 μM) and 18α-Glycyrrhetinic (25 μM) (Sigma, MO) were used to block gap junctions. Recordings were collected and analyzed using Axopatch 700B amplifier and pCLAMP10 software (Molecular Devices) and Igor 5 software (Wavemetrics Inc). Spontaneous mini-EPSCs were analyzed using mini Analysis Program (Synaptosoft Inc). At all developmental stages, the EPSC decay was best described by the sum of two exponential functions:

$$A(t)=A_{fast}(\exp(-t/\tau_{fast}))+A_{slow}(\exp(-t/\tau_{slow}))$$

where τ_{fast} and τ_{slow} are the decay time constant of the fast and slow components and A_{fast} and A_{slow} are their respective amplitudes. Data were presented as mean ± s.e.m. and statistical differences were determined using nonparametric Mann-Whitney-Wilcoxon test.

Confocal microscopy

For morphological analysis of radial clones, animals were perfused with cold PBS (pH 7.4) followed by 4% paraformaldehyde in PBS. Brains were recovered and sectioned using a Vibratome (Leica Microsystems). Sections were blocked in 10% serum and 0.1% Triton-X in PBS, and incubated with a chicken anti-GFP antibody (Aves Lab Inc) overnight at 4°C. Alexa 488-conjugated secondary antibody (Invitrogen) was then used to visualize GFP for high resolution morphological analysis. In whole-cell patch clamp recording experiments Alexa 546-conjugated biocytin was loaded onto neurons with a whole cell recording pipette, slices were fixed in 4% paraformaldehyde in PBS (pH 7.4) and biocytin was visualized with Cy3-conjugated streptavidin (Invitrogen). Z-series images were taken at 1-μm using an Olympus FV1000 confocal laser scanning microscope. Images were analyzed using FluoView (Olympus), Neurolucida (MicroBrightField, Inc.) and Photoshop (Adobe Systems).

Supplementary Material

Refer to Web version on PubMed Central for supplementary material.

Acknowledgements

We thank Drs. A. L. Joyner, J. Kaltschmidt, Y. Hayashi, and Y. Chin for comments on the manuscript; and Drs. S. C. Noctor and F. H. Gage for providing the 293gp NIT-GFP retrovirus packaging cell line; and the Shi laboratory members for insightful discussion. We are grateful for support from March of Dimes Foundation, Whitehall Foundation, Klingenstein Foundation, DANA Foundation, Autism Speaks Foundation, the NARSAD, and the NIH (to S.-H.S.).

References

1. Hubel DH, Wiesel TN. Receptive fields, binocular interaction and functional architecture in the cat's visual cortex. J. Physiol. 1962; 160:106–154. [PubMed: 14449617]
2. Mountcastle VB, Davies PW, Berman AL. Response properties of neurons of cat's somatic sensory cortex to peripheral stimuli. J. Neurophysiol. 1957; 20:374–407. [PubMed: 13439409]
3. Kozloski J, Hamzei-Sichani F, Yuste R. Stereotyped position of local synaptic targets in neocortex. Science. 2001; 293:868–872. [PubMed: 11486089]
4. Markram H, Lubke J, Frotscher M, Roth A, Sakmann B. Physiology and anatomy of synaptic connections between thick tufted pyramidal neurones in the developing rat neocortex. J. Physiol. 1997; 500(Pt 2):409–440. [PubMed: 9147328]
5. Song S, Sjostrom PJ, Reigl M, Nelson S, Chklovskii DB. Highly nonrandom features of synaptic connectivity in local cortical circuits. PLoS Biol. 2005; 3:e68. [PubMed: 15737062]
6. Thomson AM, West DC, Wang Y, Bannister AP. Synaptic connections and small circuits involving excitatory and inhibitory neurons in layers 2–5 of adult rat and cat neocortex: triple intracellular recordings and biocytin labelling in vitro. Cereb. Cortex. 2002; 12:936–953. [PubMed: 12183393]

7. Yoshimura Y, Dantzker JL, Callaway EM. Excitatory cortical neurons form fine-scale functional networks. Nature. 2005; 433:868–873. [PubMed: 15729343]
8. Yoshimura Y, Callaway EM. Fine-scale specificity of cortical networks depends on inhibitory cell type and connectivity. Nat. Neurosci. 2005; 8:1552–1559. [PubMed: 16222228]
9. Ohki K, et al. Highly ordered arrangement of single neurons in orientation pinwheels. Nature. 2006; 442:925–928. [PubMed: 16906137]
10. Ohki K, Chung S, Ch'ng YH, Kara P, Reid RC. Functional imaging with cellular resolution reveals precise micro-architecture in visual cortex. Nature. 2005; 433:597–603. [PubMed: 15660108]
11. Sato TR, Gray NW, Mainen ZF, Svoboda K. The Functional Microarchitecture of the Mouse Barrel Cortex. PLoS Biol. 2007; 5:e189. [PubMed: 17622195]
12. Maldonado PE, Godecke I, Gray CM, Bonhoeffer T. Orientation selectivity in pinwheel centers in cat striate cortex. Science. 1997; 276:1551–1555. [PubMed: 9171056]
13. Noctor SC, Flint AC, Weissman TA, Dammerman RS, Kriegstein AR. Neurons derived from radial glial cells establish radial units in neocortex. Nature. 2001; 409:714–720. [PubMed: 11217860]
14. Noctor SC, Martinez-Cerdeno V, Ivic L, Kriegstein AR. Cortical neurons arise in symmetric and asymmetric division zones and migrate through specific phases. Nat. Neurosci. 2004; 7:136–144. [PubMed: 14703572]
15. Miyata T, Kawaguchi A, Okano H, Ogawa M. Asymmetric inheritance of radial glial fibers by cortical neurons. Neuron. 2001; 31:727–741. [PubMed: 11567613]
16. Malatesta P, Hartfuss E, Gotz M. Isolation of radial glial cells by fluorescent-activated cell sorting reveals a neuronal lineage. Development. 2000; 127:5253–5263. [PubMed: 11076748]
17. Tamamaki N, Nakamura K, Okamoto K, Kaneko T. Radial glia is a progenitor of neocortical neurons in the developing cerebral cortex. Neurosci. Res. 2001; 41:51–60. [PubMed: 11535293]
18. Rakic P. Mode of cell migration to the superficial layers of fetal monkey neocortex. J. Comp. Neurol. 1972; 145:61–83. [PubMed: 4624784]
19. Rakic P. Specification of cerebral cortical areas. Science. 1988; 241:170–176. [PubMed: 3291116]
20. Kornack DR, Rakic P. Radial and horizontal deployment of clonally related cells in the primate neocortex: relationship to distinct mitotic lineages. Neuron. 1995; 15:311–321. [PubMed: 7646888]
21. Cepko CL, et al. Studies of cortical development using retrovirus vectors. Cold Spring Harb. Symp. Quant. Biol. 1990; 55:265–278. [PubMed: 2132820]
22. Walsh C, Cepko CL. Clonally related cortical cells show several migration patterns. Science. 1988; 241:1342–1345. [PubMed: 3137660]
23. Walsh C, Cepko CL. Clonal dispersion in proliferative layers of developing cerebral cortex. Nature. 1993; 362:632–635. [PubMed: 8464513]
24. Hensch TK. Critical period plasticity in local cortical circuits. Nat. Rev. Neurosci. 2005; 6:877–888. [PubMed: 16261181]
25. Micheva KD, Beaulieu C. Quantitative aspects of synaptogenesis in the rat barrel field cortex with special reference to GABA circuitry. J. Comp. Neurol. 1996; 373:340–354. [PubMed: 8889932]
26. Stern EA, Maravall M, Svoboda K. Rapid development and plasticity of layer 2/3 maps in rat barrel cortex in vivo. Neuron. 2001; 31:305–315. [PubMed: 11502260]
27. Sjostrom PJ, Turrigiano GG, Nelson SB. Rate, timing, and cooperativity jointly determine cortical synaptic plasticity. Neuron. 2001; 32:1149–1164. [PubMed: 11754844]
28. Thomson AM, Bannister AP. Interlaminar connections in the neocortex. Cereb. Cortex. 2003; 13:5–14. [PubMed: 12466210]
29. Douglas RJ, Martin KA. Neuronal circuits of the neocortex. Annu. Rev. Neurosci. 2004; 27:419–451. [PubMed: 15217339]
30. Kriegstein A, Noctor S, Martinez-Cerdeno V. Patterns of neural stem and progenitor cell division may underlie evolutionary cortical expansion. Nat. Rev. Neurosci. 2006; 7:883–890. [PubMed: 17033683]

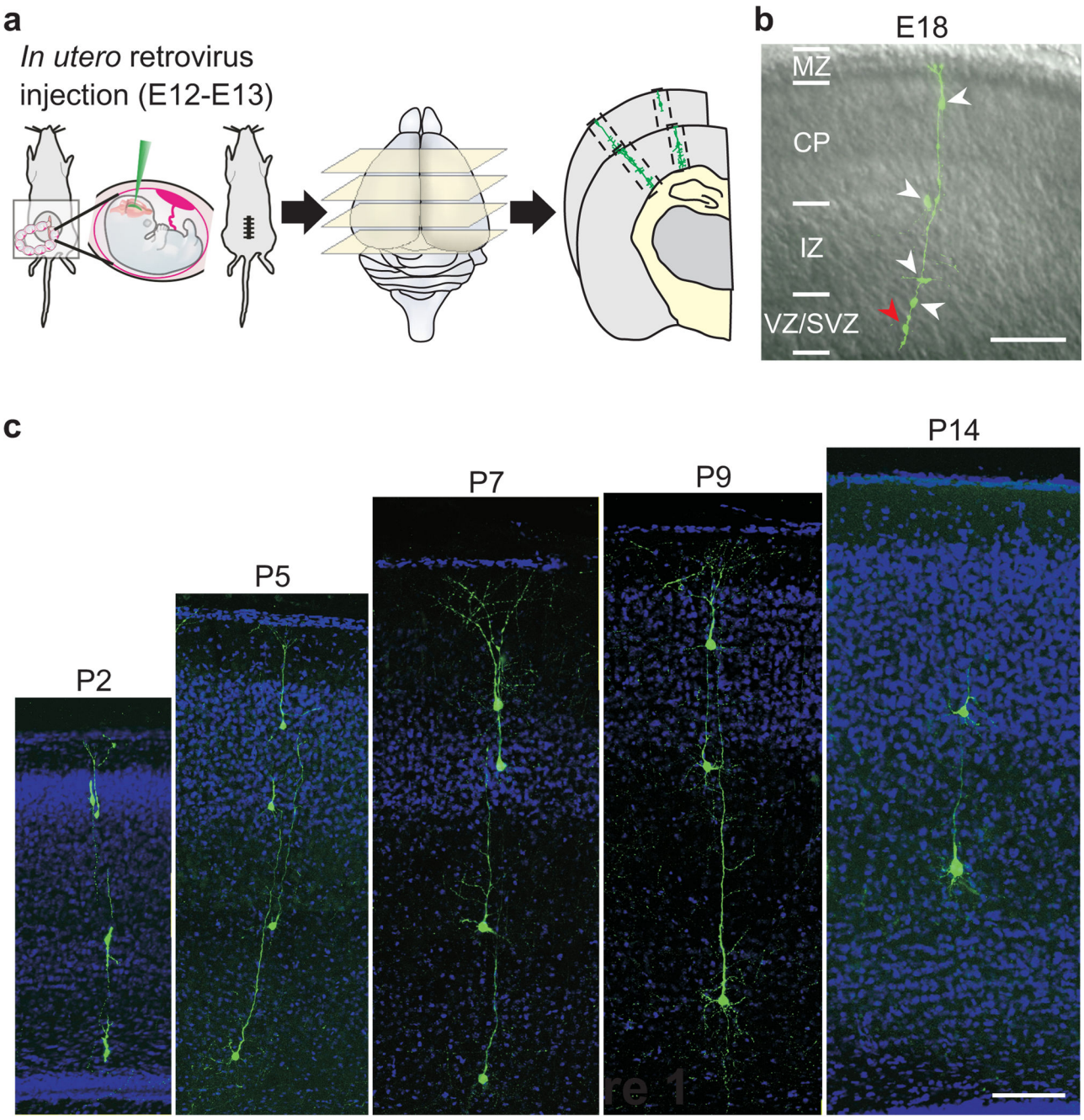

Figure 1. Morphological development of ontogenetic radial clones of excitatory neurons in the neocortex

(a) Labelling of ontogenetic radial clones in the developing neocortex with intraventricular injection of EGFP-expressing retroviruses. **(b)** An EGFP-expressing ontogenetic radial clone observed at E18 with characteristic features: one cell resembles a bipolar radial glial cell (red arrowhead) and four additional cells distribute radially along the radial glial fibre (white arrowheads). MZ, marginal zone; CP, cortical plate; IZ, intermediate zone; VZ, ventricular zone; SVZ, subventricular zone. Scale bars: 100 μm. **(c)** EGFP-expressing radial

clones observed in individual brain sections at postnatal stages. Brain sections were counterstained with a DNA dye, 4′,6-diamidino-2-phenylindole (DAPI, blue). Scale bar: 100 μm.

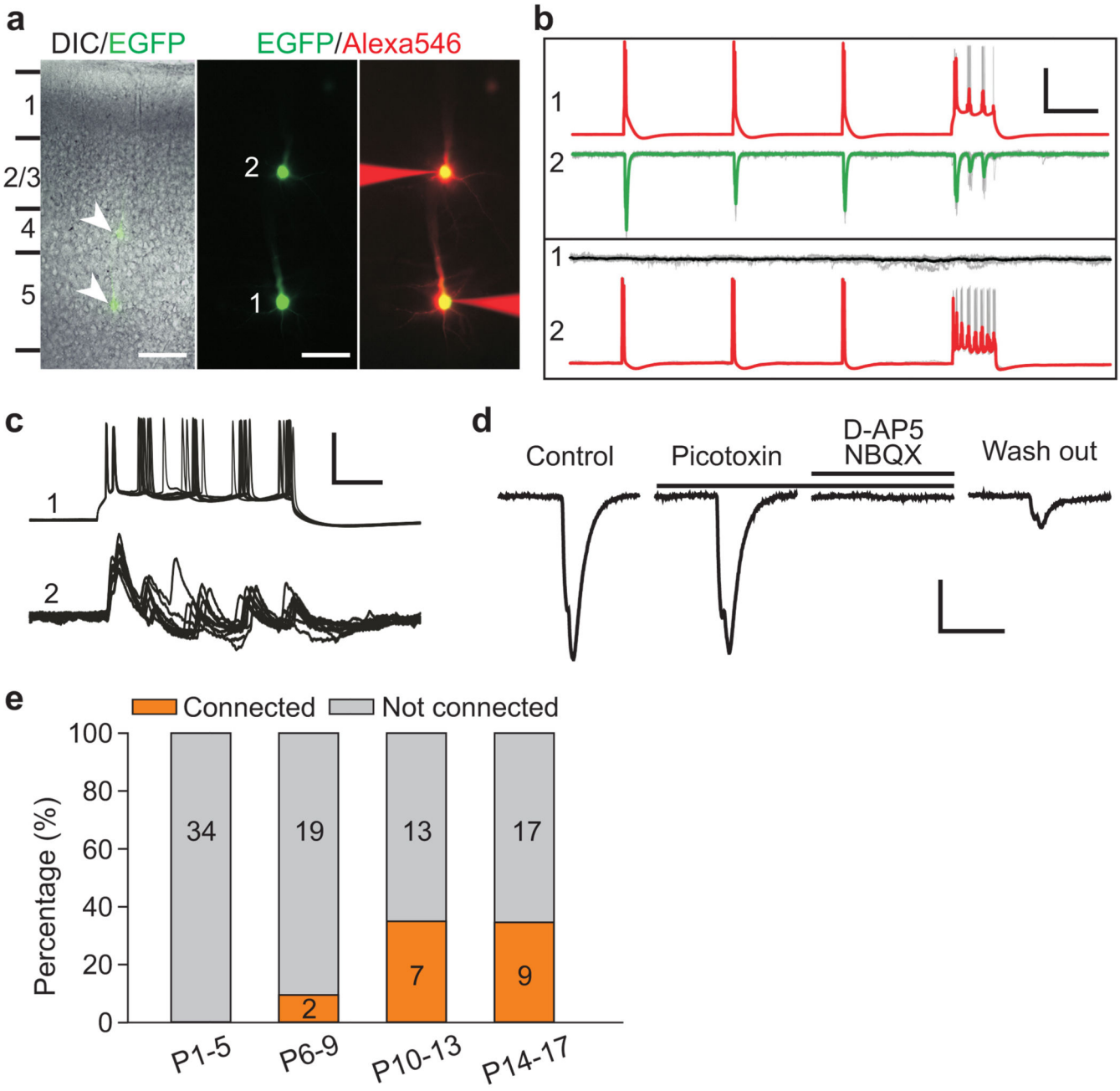

Figure 2. Synapse formation between sister excitatory neurons in ontogenetic radial clones

(a) Images of a pair of EGFP-expressing (green, middle) sister neurons in a radial clone in whole-cell configuration. Alexa 546-conjugated biocytin (red, right) was included in the recording pipette to confirm the cells being recorded and to reveal cell morphology. DIC image is shown to the left and arrows indicate two EGFP-expressing green sister neurons. Scale bars: 100 μm and 50 μm. **(b, c)** Sample traces of action potentials triggered in the presynaptic neurons (red) and EPSCs (b) or EPSPs (c) recorded in the postsynaptic neurons under voltage-clamp (b) or current-clamp (c) mode (green or black). The bold traces represent the average and the grey traces represent the individual recordings. Scale bars: 40

mV, 15 pA, and 200 msec (b); 50 mV, 1.5 mV, and 50 msec (c). **(d)** EPSC-blockage in postsynaptic neuron 2 by NBQX and D-AP5, but not by picrotoxin. Scale bar: 10 pA and 5 msec. **(e)** Summary of the rate of connectivity between sister excitatory neuron pairs in individual radial clones.

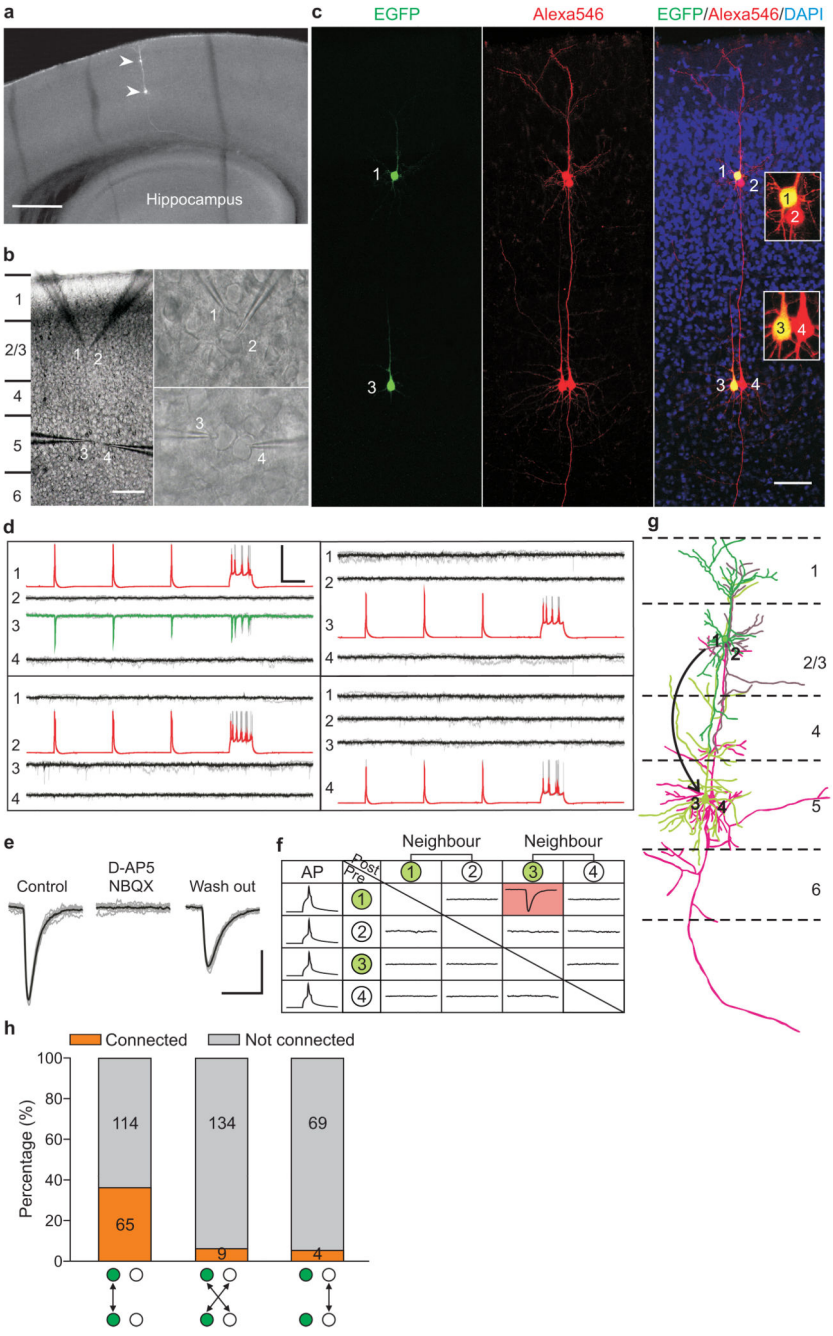

Figure 3. A strong preference for synapse formation between sister excitatory neurons in ontogenetic radial clones

(a) Image of two sister neurons in an ontogenetic radial clone in the developing neocortex. Scale bar: 1 mm. **(b, c)** DIC (b) and fluorescence (c) images of a quadruple whole-cell recording of two EGFP-expressing sister neurons (1 and 3) in *a* and two non-EGFP-expressing neurons (2 and 4) adjacent to the sisters at the same side. Scale bars: 200 μm; 100 μm. **(d)** Sample traces of action potentials (red) triggered in the presynaptic neurons and EPSCs (green and black) recorded in the postsynaptic neurons. Scale bars: 80 mV, 20 pA,

and 200 msec. **(e)** Blockage of EPSCs by NBQX and D-AP5. Scale bars: 10 pA and 5 msec. **(f)** Summary of the synaptic connection detected in this quadruple recording. Green circles indicate EGFP-expressing sister excitatory neurons and white circles indicate non-EGFP-expressing neighbouring excitatory neurons. The average traces of the postsynaptic responses are shown in the rectangle. The red-colour background indicates detection of the EPSC. Sample traces of action potentials (AP) are shown to the left. 'Pre' and 'Post' represent presynaptic and postsynaptic neurons. **(g)** Reconstruction of the neurons in this quadruple recording. The arrow indicates the detection of the synaptic connection among the four neurons. **(h)** The rate of synaptic connectivity observed between sister excitatory neurons in ontogenetic radial clones and between radially situated non-sister excitatory neurons.

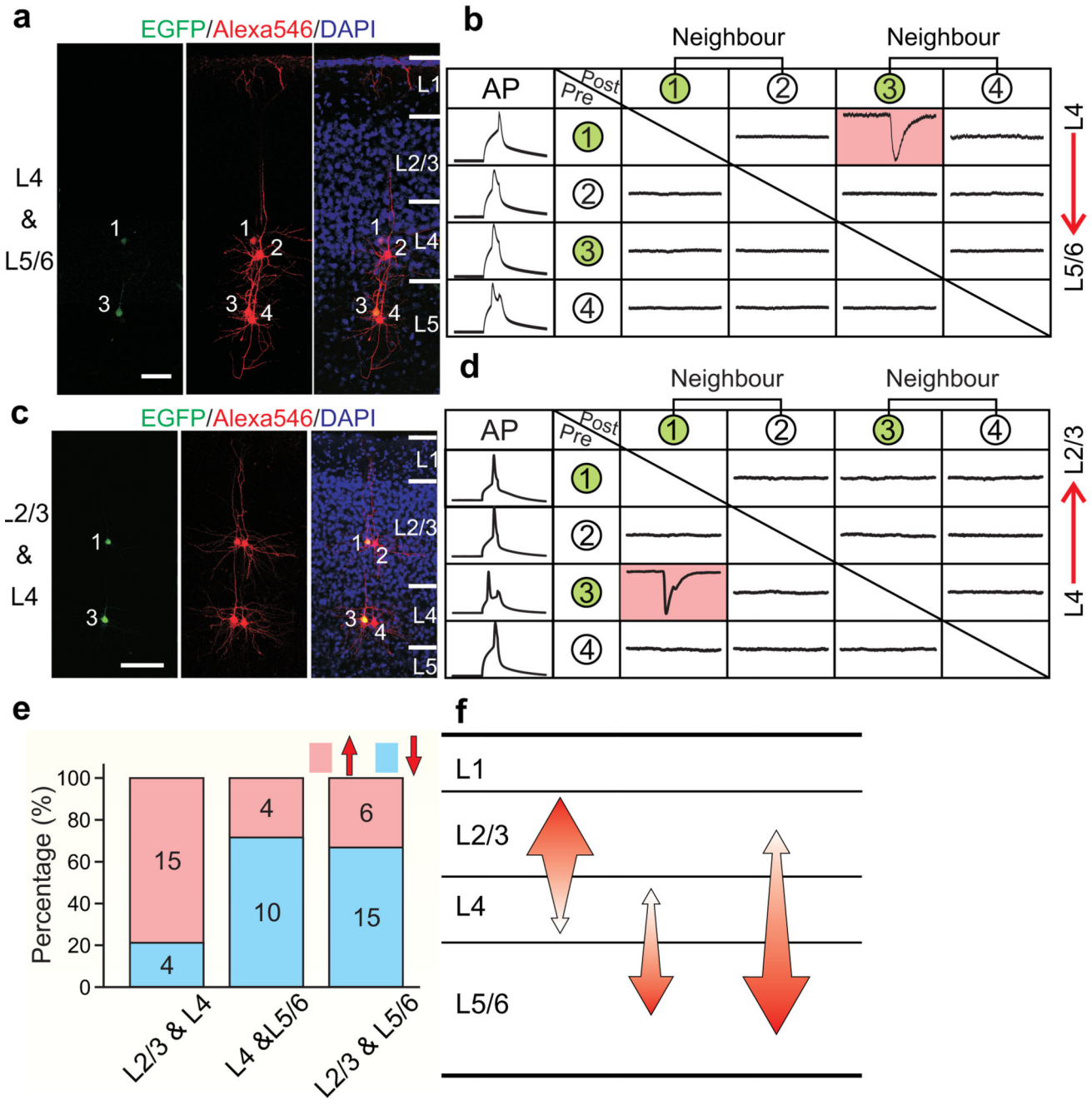

Figure 4. A highly specific microcircuit forms among sister excitatory neurons in ontogenetic radial clones

(a–d) Quadruple recording of sister excitatory neurons in individual ontogenetic radial clones located in layer 4 & layer 5/6 (a, b) or layer 2/3 & layer 4 (c, d), and their adjacent non-sister excitatory neurons. See Fig. 3 legend for details. **(e, f)** Summary of the direction of synaptic connections observed between sister excitatory neurons in individual ontogenetic radial clones. The size of the arrows in *f* reflects the abundance of the connection.